

See discussions, stats, and author profiles for this publication at: <https://www.researchgate.net/publication/8110979>

Biocompatible Lecithin Organogels: Structure and Phase Equilibria

ARTICLE *in* LANGMUIR · FEBRUARY 2005

Impact Factor: 4.46 · DOI: 10.1021/la047974f · Source: PubMed

CITATIONS

47

READS

62

7 AUTHORS, INCLUDING:



Ruggero Angelico

Università degli Studi del Molise

51 PUBLICATIONS 605 CITATIONS

SEE PROFILE



Andrea Ceglie

Università degli Studi del Molise

121 PUBLICATIONS 1,842 CITATIONS

SEE PROFILE



Giuseppe Colafemmina

Università degli Studi di Bari Aldo Moro

55 PUBLICATIONS 849 CITATIONS

SEE PROFILE



Francesco Lopez

Università degli Studi del Molise

59 PUBLICATIONS 627 CITATIONS

SEE PROFILE

Biocompatible Lecithin Organogels: Structure and Phase Equilibria

Ruggero Angelico,[†] Andrea Ceglie,[†] Giuseppe Colafemmina,^{†,‡} Francesco Lopez,[†]
Sergio Murgia,[§] Ulf Olsson,^{||} and Gerardo Palazzo^{*,‡}

*DISTAAM, Università del Molise, v. De Sanctis, I-861 00 Campobasso, Italy,
Dipartimento di Chimica, Università di Bari, v. Orabona 4, I-70126 Bari, Italy,
Dipartimento di Scienze Chimiche, Università di Cagliari, I-09042 Monserrato (CA), Italy, and
Physical Chemistry 1, Center for Chemistry and Chemical Engineering, Lund University,
P.O. Box 124, S-221 00 Lund, Sweden*

Received August 12, 2004. In Final Form: October 6, 2004

The microstructure of organogels formed upon the addition of tiny amounts of water to a solution of lecithin in fatty acid esters (viz. isopropylpalmitate and ethyloleate) was investigated by means of molecular self-diffusion measurements. In both systems lecithin and water form *disconnected* cylindrical reverse micelles. The ternary phase map for the lecithin/water/isopropylpalmitate has been investigated in detail. The organogel exists in a narrow region close to the lecithin–oil binary axis; for higher water content equilibrium between lamellae and reverse micelles is found. Lamellar phase occupies the lecithin-rich region, close to the lecithin corner (with the exception of a small island of hexagonal phase) and coexists with neat water close to the water–lecithin axis. The remaining part of the phase map shows the three-phase coexistence of water, oil, and lamellar phase.

1. Introduction

Microemulsions exhibit a rich variety of microstructures; among these the networks based on cylindrical geometries represent a challenging topic. Wormlike micelles can be entangled or interconnected, depending on the formulation of the system. Considerable theoretical effort has been devoted to the elucidation of such systems, which have been described as *living polymers*¹ or as asymmetric bicontinuous microemulsions.²

Lecithin (1,2-diacyl-*sn*-glycero-3-phosphocholine) is a ubiquitous phospholipid that accounts for more than 50% of the lipid matrix of biological membranes. Lecithin, in suitable organic solvents, forms giant cylindrical reverse micelles upon addition of small water amounts, as demonstrated by extensive studies.³ The system appears jelly-like on a macroscopic scale and is often referred to as *organogel*.⁴ On a microscopic scale, the length distribution of wormlike reverse micelles is expected to depend reversibly with intensive variables (e.g., lecithin and water concentration, temperature, and shear) in agreement with theories developed for living polymers. It has been reported that water jellifies lecithin solutions in more than 50 different organic solvents,⁵ but structural investigations have only been performed on systems based on hydro-

carbons, viz., cyclohexane, isooctane, and decane; for reviews see refs 6, 7, and 8.

On the applied research perspective, the rich phase behavior exhibited by surfactant systems is very promising in the field of drug delivery.⁹ The most significant problem associated with formulating microemulsions for pharmaceutical use is the difficulty associated with excipient acceptability. The largest part of our knowledge on surfactant self-assembly is related to systems made of surfactants, which do not have regulatory approval for use in pharmaceutical products. Being a natural phospholipid, lecithin represents a notable exception and, indeed, lecithin-based organogels (prepared with suitable oils) have been successfully proposed as drug delivery systems.^{10–16} Detailed structural investigations on the self-assembled aggregates made by lecithin in biocompatible oils are, however, still lacking. In the present paper we report on the microstructure of lecithin organogels made of biocompatible fatty acid esters (viz., isopropylpalmitate and ethyloleate) and extend our previous phase behavior investigations^{19,27} to the lecithin/water/isopropylpalmitate system.

* To whom correspondence may be addressed. E-mail: palazzo@chimica.uniba.it.

[†] Università del Molise.

[‡] Università di Bari.

[§] Università di Cagliari.

^{||} Lund University.

(1) Cates, M. E.; Candau, S. J. *J. Phys.: Condens. Matter* **1990**, *2*, 6869 and references therein.

(2) Tlusty, T.; Safran, S. A.; Strey, R. *Phys. Rev. Lett.* **2000**, *84*, 1244.

(3) Tlusty, T.; Safran, S. A. *J. Phys.: Condens. Matter* **2000**, *12*, A253.

(4) Schurtenberger, P.; Jerke, G.; Cavaco, C.; Pedersen, J. S. *Langmuir* **1996**, *12*, 2433 and references therein.

(5) Scartazzini, R.; Luisi, P. L. *J. Phys. Chem.* **1989**, *92*, 829.

(6) Luisi, P. L.; Scartazzini, R.; Haering, G.; Schurtenberger, P. *Colloid Polym. Sci.* **1990**, *268*, 356.

(6) Shchipunov, Y. A. *Colloid Surf., A* **2001**, *183–185*, 541 and references therein.

(7) Schurtenberger, P. *Chimia* **1994**, *48*, 72.

(8) Palazzo, G.; Angelico, R.; Ceglie, A.; Olsson, U. In *Self-Assembly*; Robinson, B., Ed.; IOS Press: Burke, VA, 2003; p 318.

(9) Lawrence, M. J.; Rees, G. D. *Adv. Drug Delivery Rev.* **2000**, *45*, 89.

(10) Kreilgaard, M. *Adv. Drug Delivery Rev.* **2002**, *54* (Suppl. 1), S77.

(11) Willman, H.; Walde, P.; Luisi, P. L.; Gazzaniga, A.; Stroppolo, F. *J. Pharm. Sci.* **1991**, *81*, 871.

(12) Walde, P.; Dreher, F. In *Tissues Cultures in Cosmetics Biotechnology*; Gambari, R.; Nastruzzi, C., Eds.; A. Nocenti: Ferrara, 1992; p 65.

(13) Papantoniou, I.; Müller-Goymann, C. C. *Pharm. Pharmacol. Lett.* **1995**, *5*, 28.

(14) Nastruzzi, C.; Gambari, R. *J. Controlled Release* **1994**, *29*, 53.

(15) Müller-Goymann, C. C.; Hamann, H. J. *J. Controlled Release* **1993**, *23*, 165.

(16) Bonina, F. P.; Montenegro, L.; Scrofani, N.; Esposito, E.; Cortesi, R.; Menegatti, E.; Nastruzzi, C. *J. Controlled Release* **1995**, *34*, 53.

(17) Dreher, F.; Walde, P.; Walther, P.; Weherli, E. *J. Controlled Release* **1997**, *45*, 131.

2. Materials and Methods

Soybean lecithin (Epikuron 200) was a generous gift from Degussa Bioactives AG and consists of soybean *phosphatidylcholine* (PC) with a purity of 95% and with an average molecular weight of 772 Da. The lecithin used in this work is of the same brand as used in most of the published investigations of lecithin organogels. As in previous works, it was used without further purification, which consequently means that it is a certain mixture of phosphatidylcholines of different chain lengths and degree of saturation.¹⁷ Depending on the batch and on storage conditions, the water content of soybean lecithin ranges between 0.3 and 1 molecules of water per PC molecule.¹⁸ In the present work all water contents are expressed in terms of water added to the sample. Isopropylpalmitate (hexadecanoic acid isopropyl ester) of purity >90.0% was obtained from Fluka Chemika and ethyloleate (octadec-9-enoic acid ethyl ester) of purity >98.0% was obtained from Sigma-Aldrich. Both oils were used as received. Water was twice distilled in an all-quartz device.

Microscopy with polarized optics (crossed polarizer and analyzer) and small-angle X-ray scattering (SAXS) measurements were performed as described in ref 19. The measurements of water and lecithin self-diffusion coefficients via pulsed gradient spin-echo (PGSE) NMR were performed on a Bruker Avance 300 MHz (7.05 T) spectrometer equipped with a Bruker field gradient probe that can reach field gradients of 300 G/cm. A typical experiment was performed by keeping the gradient pulse length δ constant and gradually increasing the gradient strength g . For water self-diffusion experiments a normal Hahn echo sequence was used. Since the lecithin reverse micelles are large, the slow reorientation of the aggregates makes the T_2 relaxation of the surfactant quite rapid. For this reason, the lecithin self-diffusion measurements were carried out using a stimulated echo sequence. For each gradient strength, 16 phase cycling steps were accumulated in order to remove unwanted echoes. The resonance intensities of the methyl groups at 3.5 ppm of the $-N^+-(CH_3)_3$ of the lecithin headgroup were used in the evaluation of the surfactant self-diffusion experiments.

Viscosity measurements were performed on a Physica UDS 200 rheometer using a cone-plate geometry (25 mm, 2°). The viscosity was evaluated from the slope of shear stress (σ) against shear rate ($\dot{\gamma}$) plot in continuous shear measurements.

Samples were prepared by weighing appropriate amounts of lecithin, water, and oil into glass tubes with screw caps. The samples were mixed by repeated centrifugation or shaking (depending on their viscosity) at regular intervals for approximately 2 weeks. Then, they were left to stand for at least 1 week at 25.0 ± 0.2 °C in a water bath thermostat before viscosity or PGSE-NMR measurements. Samples for the phase diagram determination were allowed to ripen, in the dark, for several months in a room at 25 ± 4 °C for most of the time and finally allowed to stand in a water bath at 25.0 ± 0.2 °C for 4 weeks.

The following notation will be used below for the sake of shortness: W_0 = mole ratio water/lecithin; lecithin = PC; isopropylpalmitate = IPP; ethyloleate = EO; H = hexagonal phase; L_a = lamellar phase; L_2 = microemulsion phase made of *disconnected* reverse micelles.

In the calculation of volume fractions we have used the following densities: IPP density = 0.853 g/mL; EO density = 0.87 g/mL; PC density = 1.0198 g/mL.

3. Results

3.1. Rheological Behavior. Lecithin solutions in isooctane, cyclohexane, and decane become very viscous upon addition of tiny amounts of water.^{4,20} This fact suggests the systems share a similar microstructure. Such a deduction was confirmed by a decade of small-angle neutron scattering (SANS) studies ascertaining that the

organogels bear the same *short scale* microstructure: cylindrical reverse micelles.^{21,22} The description of microstructure on a longer length scale appears to be very delicate: evidence of branched networks have been reported for the isooctane-^{23,24} and decane-based⁶ systems, while with cyclohexane as oil, no branches could be detected.²⁵ The dependence of the viscosity, η , on W_0 has been studied in some detail only in lecithin gels with hydrocarbons.^{4,6,20} At constant lecithin concentration with increasing water loading, cylindrical reverse micelles grow and entangle thus forming a network that produces an increase in the viscosity. If the zero-shear viscosity of the organogel is measured versus water addition, a maximum viscosity is generally reached at a given W_0 value. Further hydration results in a gradual decrease in η until a phase separation is obtained. The shape of the η vs W_0 plot and the kind of phase separation seems to be related to the degree of connectivity of the cylindrical reverse micelles. Indeed, in the presence of branches between micelles, the decrease in viscosity is accounted for by a water-induced increase in the branch point density (branch points can slide along the micellar contour)²⁶ and, for a water content high enough ($W_0 \sim 5$), the fully connected network collapses expelling excess oil. Such a situation is met for isooctane²⁰ and decane⁶ organogels, and in these cases the decrease in viscosity is interrupted by the phase boundary before very low η values are attained.²⁷ On the contrary, in cyclohexane organogels the η -dependence on W_0 displays a symmetrical shape and the viscosity diminishes back to values typical of a dispersion of hard spheres.²⁸ In this last case the drop in viscosity is due to a rod-to-sphere shape transition of *disconnected* reverse micelles,²⁹ and finally, for further water addition ($W_0 \sim 22$), the system expels excess water leading to a Winsor II equilibrium between excess water and spherical droplets of the optimal size.¹⁹

Lecithin organogels made of fatty acid esters have been proposed to deliver pharmaceuticals, but a detailed structural investigation is still lacking. Continuous shear experiments (σ vs $\dot{\gamma}$) performed on organogels prepared with IPP and EO demonstrate that the viscosity is independent of the shear rate in the range $1 \text{ s}^{-1} \leq \dot{\gamma} \leq 500 \text{ s}^{-1}$ (not shown). The rheological behavior of organogels prepared with hydrocarbons was previously found to be very different. The viscosity of cyclohexane based system³⁰ drops for $\dot{\gamma} > 0.35 \text{ s}^{-1}$, while with isooctane³⁰ and decane³¹ as oil, shear-thinning is found when $\dot{\gamma}$ exceeds $\sim 10 \text{ s}^{-1}$. Figure 1 shows the dependence of the viscosity on the water-to-lecithin mole ratio (W_0) for organogels prepared with IPP and EO (the concentration of lecithin is 15 wt %). For both the solvents a moderate increase in the W_0

(21) Schurtenberger, P.; Magid, L. J.; King, S. M.; Lindner, P. *J. Phys. Chem.* **1991**, *95*, 4173.

(22) Jerke, G.; Pedersen, J. S.; Egelhaaf, S. U.; Schurtenberger, P. *Physica B* **1997**, *234–236*, 273.

(23) Ambrosone, L.; Angelico, R.; Ceglie, A.; Olsson, U.; Palazzo, G. *Langmuir* **2001**, *17*, 6822.

(24) Cirkel, P. A.; van der Ploeg, J. P. M.; Koper, G. J. M. *Phys. Rev. E* **1998**, *57*, 6875. Cirkel, P. A.; Fontana, M.; Koper, G. J. M. *J. Dispersion Sci. Technol.* **2001**, *2–3*, 211.

(25) Angelico, R.; Olsson, U.; Palazzo, G.; Ceglie, A. *Phys. Rev. Lett.* **1998**, *81*, 2823.

(26) Appel, J.; Porte, G.; Khatory, A.; Kern, F.; Candau, S. J. *J. Phys. II* **1992**, *2*, 1045.

(27) Angelico, R.; Ceglie, A.; Colafemmina, G.; Delfino, F.; Olsson, U.; Palazzo, G. *Langmuir* **2004**, *20*, 619.

(28) Schurtenberger, P.; Magid, L. J.; Lindner, P.; Luisi, P. L. *Prog. Colloid Polym. Sci.* **1992**, *89*, 274.

(29) Angelico, R.; Ceglie, A.; Cirkel, P. A.; Colafemmina, A.; Giustini, M.; Palazzo, G. *J. Phys. Chem. B* **1998**, *102*, 2883.

(30) Cavaco, M. C. Ph.D. Thesis, Zürich, 1994, Diss. ETH No. 10897, Chapter B.3.

(31) Shchipunov, Y. A.; Hoffmann, H. *Rheol. Acta* **2000**, *39*, 542.

(17) Shinoda, K.; Araki, M.; Sadaghiani, A. S.; Khan, A.; Lindman, B. *J. Phys. Chem.* **1991**, *95*, 989.

(18) Scartazzini, R. Ph.D. Thesis, ETH Zurich, Nr. 9186, 1990.

(19) Angelico, R.; Ceglie, A.; Olsson, U.; Palazzo, G. *Langmuir* **2000**, *16*, 2124.

(20) Schurtenberger, P.; Scartazzini, R.; Luisi, P. L. *Rheol. Acta* **1989**, *28*, 372.

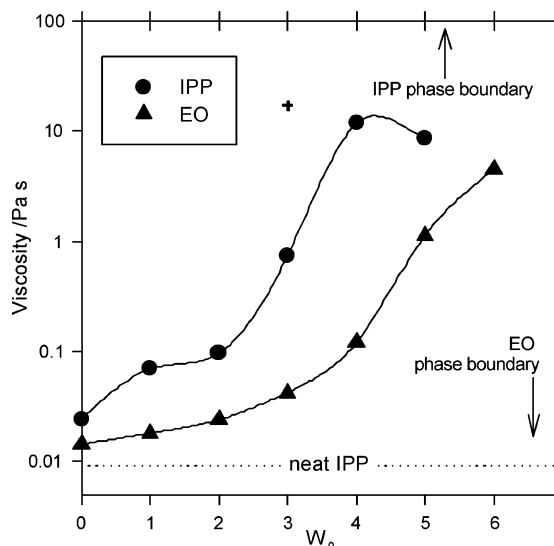


Figure 1. Viscosity of organogels prepared with IPP and EO as a function of W_0 . Conditions: $T = 25\text{ }^\circ\text{C}$; samples (1 month old) were prepared by water dilution of a lecithin/oil mixtures (PC = 15 wt %). Also shown are the boundaries of single-phase regions (arrows) and the viscosity of neat IPP (dotted line). For the purpose of comparison, the viscosity value reported in ref 4 for IPP at a similar lecithin content is shown as a plus sign.

parameter (up to $W_0 = 5$ and $W_0 = 6$ for IPP and EO, respectively) induces an increase of approximately 3 orders of magnitude in the macroscopic viscosity ($\eta \sim 10\text{ Pa}\cdot\text{s}$). Our results on IPP are in reasonable agreement with the viscosity measured at $W_0 = 3$ by means of oscillatory measurements⁴ (shown as a plus sign in Figure 1).

For the purpose of comparison we recall that, at comparable lecithin volume fraction, the maximum value of viscosity is around $10^3\text{ Pa}\cdot\text{s}$ when the hydrocarbons are used as oil.^{4,7,30,31} The viscosity measured for the EO-based organogels is systematically lower than that found when IPP is used as oil (at given W_0). Since the measured viscosity of the neat oils (η°) are mutually close ($\eta^\circ = 9.22\text{ mPa}\cdot\text{s}$ for IPP and $\eta^\circ = 8.45\text{ mPa}\cdot\text{s}$ for EO) such a difference likely reflects some differences in microstructure. We have estimated that the maximum water uptake by the organogel is around $W_0 = 5.2$ for IPP and $W_0 = 6.6$ for EO. As shown in Figure 1 the phase boundaries for both the oils are so close to the η -maximum that any decrease in viscosity is hardly discernible.

3.2. Organogels Microstructure: Aggregate's Branch Density, Size, and Shape. We can gain insight on the structure of organogels by probing the molecular motion of lecithin and water by means of pulsed gradient spin-echo (PGSE) NMR.³² Briefly, one monitors the ^1H echoes upon application of a couple of magnetic field gradients of duration δ and strength g . As accounted in detail elsewhere^{33,34} the echo intensity, $I(K)$, decreases with the gradient intensity δg , and for unrestricted (Brownian) diffusion the echo intensity is described by

$$I(K) = I(0) e^{-KD} \quad (1)$$

where D is the self-diffusion coefficient of the spin-bearing species and $K = \gamma^2 g^2 \delta^2 (\Delta - \delta/3)$. Here γ is the gyromagnetic ratio for the proton and the time interval between the two

Table 1. Diffusion Properties of Water and PC in Organogels Made of IPP and EO^a

oil	W_0	PC = 5%		PC = 15%	
		$D_{\text{lec}}/\text{m}^2\text{ s}^{-1}$	$D_{\text{water}}/\text{m}^2\text{ s}^{-1}$	$D_{\text{lec}}/\text{m}^2\text{ s}^{-1}$	$D_{\text{water}}/\text{m}^2\text{ s}^{-1}$
IPP	0.0	1.15×10^{-11}		7.69×10^{-12}	
IPP	2.1	4.55×10^{-12}		2.10×10^{-12}	
IPP	3.0	2.54×10^{-12}	1.34×10^{-10}	3.00×10^{-12}	0.64×10^{-10}
IPP	4.1	8.34×10^{-13}	1.50×10^{-10}	1.13×10^{-13}	0.75×10^{-10}
IPP	5.4 ^b	1.76×10^{-13}	1.27×10^{-10}	5.20×10^{-11}	1.13×10^{-10}
EO	1.8	1.2×10^{-11}			
EO	2.8	9.5×10^{-12}			
EO	4.4	5.3×10^{-12}			
EO	5.7	1.64×10^{-12}	1.7×10^{-10}		
EO	6.8 ^b	4.6×10^{-12}			

^a Samples were prepared by water dilution of PC-oil mixtures

^b Phase separated sample, the data refer to the upper isotropic phase only.

gradients, Δ , represents the experiment time scale. For self-assembled aggregates with a size smaller than the diffusion length (defined as $(2D\Delta)^{1/2}$) eq 1 is expected to apply. At variance, if one of the aggregate dimensions becomes comparable with the diffusion length and the lifetime of the spin-bearing molecule in the aggregate is long enough, the molecular displacement *inside* the aggregate contributes to the overall molecular motion and a deviation from eq 1 is expected.³⁵ In particular, in lecithin organogels made of hydrocarbons the lecithin diffusion along the contour of wormlike reverse micelles was found to deeply influence the echo attenuation that becomes nonexponential (see refs 25 and 23). A signature of this situation is a dependence on Δ of the echo attenuation in a $I(K)$ vs K plot. It should be noticed that for interconnected wormlike micelles the lateral diffusion of surfactant gives rise to exponential echo attenuation if the density of branch points is high enough. For this reason we have focused PGSE-NMR measurements on dilute samples (PC = 5 wt %) where the density of interconnections is expected to be low.²³ We found, for both EO and IPP, that all the echo attenuations were found to be *independent of time scale*, in the range 20–300 ms explored, thus demonstrating that the diffusion on this time scale is described by Gaussian statistics with a single, well-defined, diffusion coefficient. The lecithin self-diffusion coefficients (D_{lec} listed in Table 1) are low (10^{-11} to $10^{-13}\text{ m}^2\text{ s}^{-1}$) and strongly decrease upon water loading (see Figure 2). This finding definitively rules out the presence of connections among micelles, because theory foretells an increase in branch density upon water loading³⁶ and a consequent increase in the surfactant diffusion up to a plateau corresponding to one-third of the lateral diffusion coefficient.³⁵ For the purpose of comparison, in Figure 2 are also shown the results previously obtained in the branched system PC/water/isooctane, where the increase in the apparent D_{lec} , upon water loading, reflects an increase in branch density (see ref 23 for details). As a whole the data of Table 1 and Figure 2 suggest that the D_{lec} measured by means of PGSE-NMR coincides with the self-diffusion coefficient of aggregates growing in size upon water addition. Furthermore, the D_{lec} values are hardly consistent with spherical reverse micelles. Actually, for (monodisperse) spherical water-in-oil (w/o) droplets the radius of the aqueous core depends on the water volume fraction (ϕ_w) as $R_{\text{wc}} = 3l_s\phi_w/\phi_s$, where ϕ_s is the surfactant volume fraction and l_s is the

(32) Stilbs, P. *Prog. NMR Spectrosc.* **1987**, *19*, 1.

(33) Stejskal, E. O.; Tanner, J. E. *J. Chem. Phys.* **1965**, *42*, 288.

(34) Stilbs, P.; Moseley, M. E.; Lindman, B. *J. Magn. Reson.* **1980**, *40*, 401.

(35) Callaghan, P. T. *Principles of Nuclear Magnetic Resonance Microscopy*; Clarendon Press: Oxford, 1991; Chapter 7.

(36) Zilman, A. G.; Safran, S. A. *Phys. Rev. E* **2002**, *66*, article no. 051107.

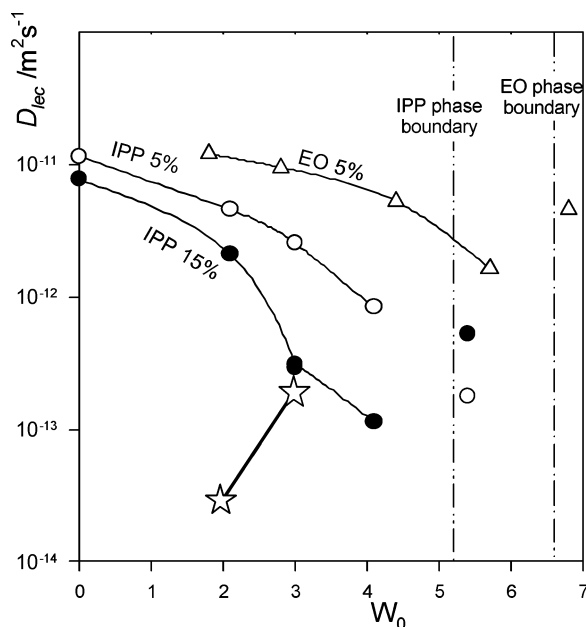


Figure 2. W_0 dependence of the lecithin self-diffusion coefficients. Samples (1 month old) were prepared by water dilution of lecithin/oil mixtures. Open triangles denote EO gels at PC = 5 wt %; open and closed circles denote IPP gels (with PC = 5 and 15 wt %, respectively). Also shown are the locations of the phase boundaries. For the purpose of comparison, also shown, as stars, are the apparent self-diffusion coefficients of lecithin observed in the PC/water/isooctane system (from ref 23).

surfactant size (around 25 Å for the lecithin),³⁷ and the overall radius $R \approx l_s + R_{wc}$ becomes

$$R \approx l_s \left(1 + 3 \frac{\phi_w}{\phi_s} \right) \quad (2)$$

Therefore, on the basis of the low values of the ratio ϕ_w/ϕ_s we expect, upon increase in W_0 from 0 to 6.8, an almost negligible swelling for spherical micelles (from 24 to 35 Å). In Figure 3 the prediction of the above equation (dashed line) is compared with the apparent hydrodynamic radius obtained by applying the Stokes–Einstein relation to the D_{lec} values of Figure 2. Despite the agreement found at very low water content, the prediction for spherical aggregates is incompatible with the measured hydrodynamic radii. On the other hand, water-induced monodimensional growth of strongly anisotropic aggregates consistently accounts for the diffusional behavior and for the high viscosity of the samples. On the basis of these arguments and in analogy with the investigations performed on hydrocarbon-based organogels, we retain that the reverse micelles in organogels made of fatty acids esters are disconnected (i.e., a true L_2 phase) and cylindrical in shape. This holds also at the high concentration used in viscosity measurements as shown in Figure 2 (at least in the case of IPP-based gels). It is clear that, at fixed W_0 , an increase in lecithin concentration induces a dramatic increase in hydrodynamic size of the micelles (see Figure 3).

It should be noticed that the micellar sizes measured with IPP as oil are systematically higher than those found in EO-organogels (Figure 3). This suggests that the cylindrical micelles are longer in IPP than in EO and furnish a rationale for the differences in viscosity between the two systems (Figure 1).

(37) At low W_0 , the repeat distance (twice the length of a PC molecule) found in the L_a phase is around 50 Å (Table 2).

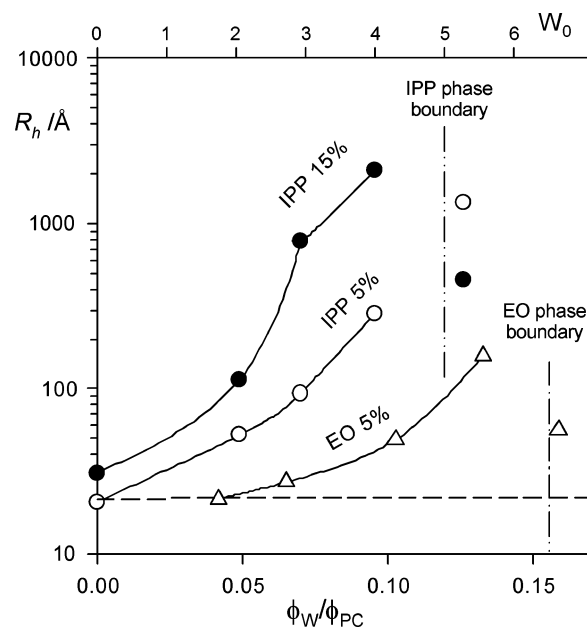


Figure 3. Micellar size as a function of the volume ratio ϕ_w/ϕ_s (lower axis) and of W_0 (upper axis). Dashed straight line is the prediction of eq 2; points are the apparent hydrodynamic radii (R_h) evaluated from the self-diffusion coefficients of Figure 2 according to $R_h = KT/6\pi\eta^\circ D_{lec}$ (K = Boltzmann's constant). Symbols are the same as those given in Figure 2. Also shown are the locations of the phase boundaries.

The oil self-diffusion coefficient is almost constant (1.3×10^{-10} to $1.5 \times 10^{-10} \text{ m}^2 \text{ s}^{-1}$) and independent from water and lecithin loading. On the contrary, the water self-diffusion coefficients (D_{water} , listed in Table 1) are dependent on the lecithin concentration. At low lecithin loading D_{water} shares about the same value of the self-diffusion coefficient of oil but becomes systematically lower at higher lecithin concentration. Such a behavior could be explained by assuming the partition of water between aggregates and oil as previously clarified in the case of isooctane-²³ and cyclohexane-based⁸ organogels, but this point was not investigated in detail in the present case.

3.3. Phase Equilibria. A crucial point in the use of microemulsions as drug delivery systems is their behavior in contact with the large volume of body fluids. This step is extremely delicate when dealing with w/o microemulsions. Actually, despite the huge amount of studies, the fate of a *generic* w/o microemulsion upon addition of large water amounts is still unpredictable. This is true also for PC/water/oil systems. Indeed, upon water dilution, cyclohexane-organogels show a Winsor II phase separation,¹⁹ while decane- and isooctane-based organogels show an equilibrium between interconnected micellar network and pure oil.²⁷ In the case of both IPP- and EO-based systems, we have found that water loading results, above a critical hydration, in a phase separation between a birefringent liquid-crystalline phase and a less dense isotropic phase. The isotropic phase is not very viscous (the same viscosity of neat oil, as judged by eye) and contains lecithin and water. PGSE-NMR experiments on this isotropic phase give essentially the same results obtained on single-phase gels (see Table 1). The main difference is the low intensity of NMR signals due to dilution, and we identify this phase as a dilute L_2 phase. The dense phase reveals, when observed between crossed polarizers, textures usually associated with a *lamellar* (L_a) phase (sample a, Figure 4). SAXS spectra are characterized by a sharp first-order Bragg peak followed by weaker reflections consistent with lamellar order (Figure 5, curve a). For further water

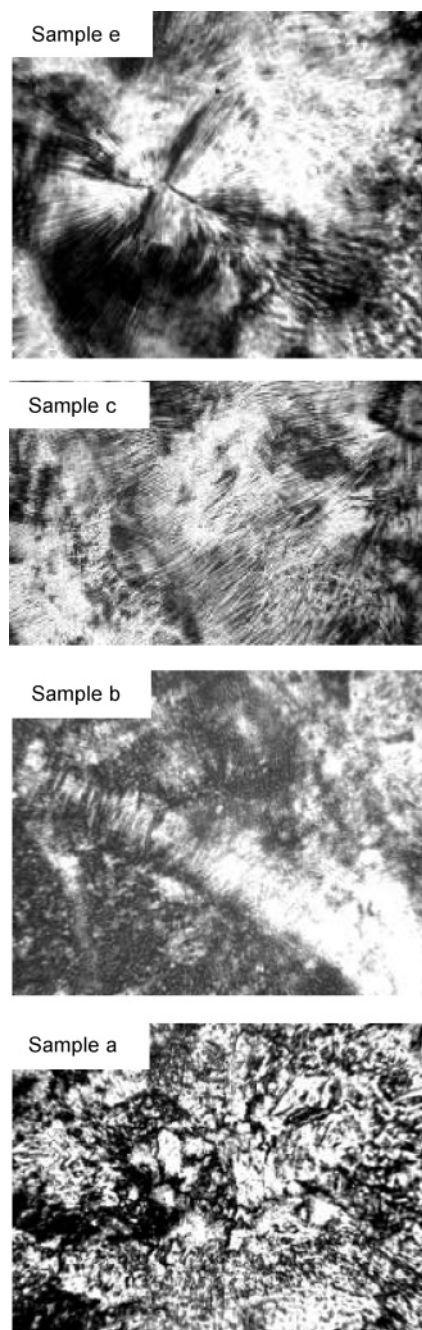


Figure 4. Birefringence textures recorded in the liquid crystalline phases for the PC/water/IPP system at 25 °C (magnification 28 \times): (a) lamellar phase of a sample in coexistence with L_2 phase; (b) pure lamellar phase; (c) fanlike texture of pure reversed hexagonal phase; (d) lamellar and hexagonal textures in a three-phase sample in equilibrium with L_2 . The images were recorded after 2 years of ripening.

addition the biphasic system becomes milky and viscous resembling an emulsion, sometime in equilibrium with excess oil. Observation with a microscope does not reveal water droplets but does show some “holes” (defects) on a rugged background (Figure 6A). When the sample is observed between crossed polarizers, the background reveals birefringence texture typical of lamellar structures while the “holes” are dark (Figure 6B). These features, and the presence of excess oil, suggest that the emulsion-like sample is made by lamellar liquid crystal embedding mesoscopic oil domains, a situation drastically different from the water-in-oil emulsions encountered by using hydrocarbons as oils. Therefore, the short-time phase

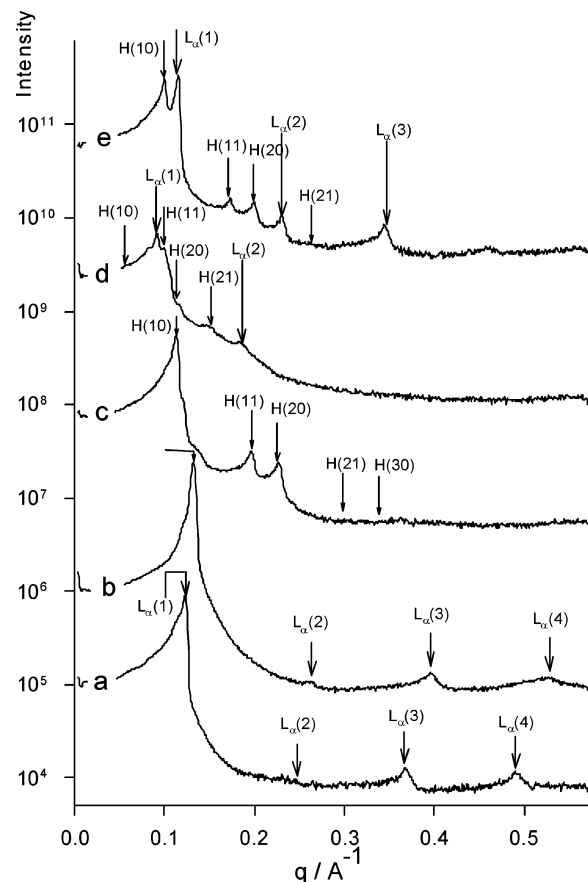


Figure 5. SAXS curves of representative samples of the PC/water/IPP system. The location of samples in the phase map is shown in Figure 7. Also shown are the position of reflections according to fit to lamellar (L_α) and hexagonal (H) order. The measurements were performed after 2 years of ripening.

behavior upon water dilution of fatty acid esters appears to be different from that found for lecithin in hydrocarbons. To have insight on this point we have undertaken a systematic study in the case of the PC/water/IPP system. A large number (92) of samples has been prepared and allowed to ripen for a long time (2 years). The resulting phase map is presented in weight fraction in Figure 7, and the results from SAXS experiments on a number of selected samples are listed in Table 2. The organogel (isotropic L_2 phase) exists in a narrow water-lean region of the phase diagram close the binary PC–IPP axis. For $W_0 > 5$ the system phase separates into a dilute reverse micellar solution and L_α phase. In the L_2 phase, the water and PC signals in NMR spectra becomes weaker and weaker upon water loading, indicating that along water dilution the L_α phase becomes more concentrated at the expense of L_2 phase. All the above-mentioned findings manifest themselves on a time scale of 1 day to 1 month. Further addition of water turned the system to the emulsion-like samples as described above. After a few months of ripening the samples reveal a phase separation of spherulites, oil, and water. Longer ripening (up to 2 years) does not change the fate of the system. Spherulites are easily recognized with polarized optics microscopy by the maltese cross textures (a representative example is shown in Figure 8). They are arranged in the form of closed multilamellar vesicles that in lecithin systems, usually, represent nonequilibrium arrangement of the L_α phase. This means that for high enough water loading, all the lecithin self-assembles into lamellar structures that can incorporate only limited amounts of oil and water. The

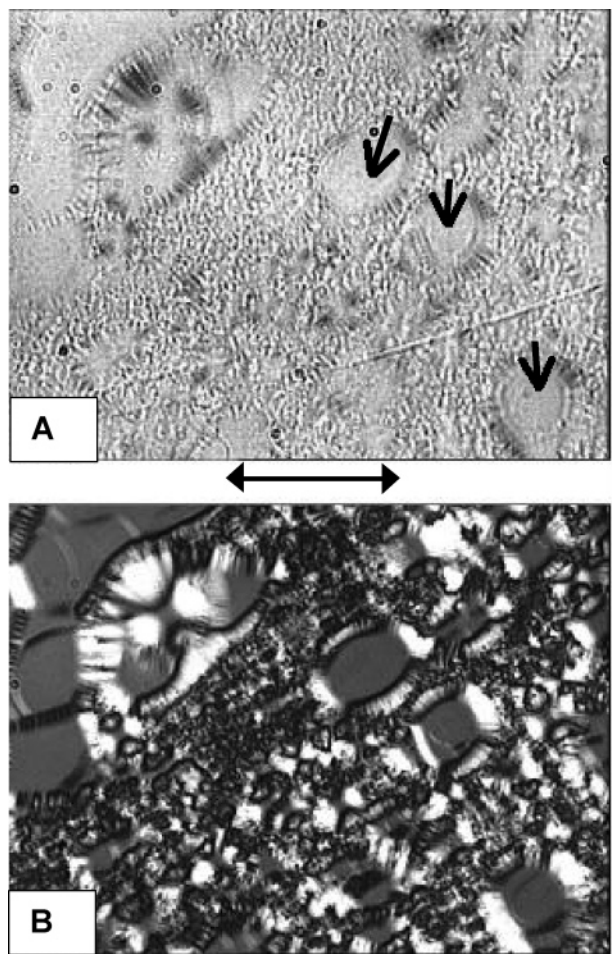


Figure 6. Micrographs of emulsion-like sample: (plate A) micrograph with nonpolarized light, arrows indicate holes in the rugged background; (plate B) same as in A but observed through crossed polarizers, note the dark (isotropic) appearance of the holes. Conditions: PC = 27.8 wt %; IPP = 64.9 wt %; $W_0 = 11.3$; $T = 25^\circ\text{C}$; pictures were taken 1 week after sample preparation. The bar corresponds to 10 μm .

SAXS curves of spherulites show two very broad correlation peaks whose intensities increased with increasing lecithin concentration (Figure 8). The lattice spacing calculated from the position of those peaks gave 70 Å and is independent from the water and oil content (Figure 8, consistent with the presence of excess solvent). At high lecithin concentrations in the L_α , no spherulites were observed (see sample b in Figures 4 and 5). For approximately equal amounts of water and oil and high lecithin content, a small “island” of an hexagonal phase is found (see sample c in Figures 4 and 5). The hexagonal island is connected to the two-phase $L_\alpha + L_2$ region by a multiphase region that was not investigated in every detail (dark gray area in Figure 7). We have found two-phase $L_\alpha + H$ (e.g., sample d) and three-phase $L_2 + H + L_\alpha$ (e.g., sample e) samples, but the phase boundaries between these domains have not been determined.

4. Discussion

Special care must be taken to avoid kinetic artifacts when studying the phase behavior of phospholipid systems. For this reason the phase diagram (Figure 7) was drawn on the basis of the observation of 2-year old samples. A contraindication of this procedure is that both PC and IPP can undergo chemical modification (e.g., hydrolysis). However, the main features of the phase diagram of Figure

7 manifest themselves on a relatively short time scale. Single-phase organogels (L_2) and the two-phase region $L_2 + L_\alpha$ are recognized within 1 day from sample preparation. Samples with a liquid crystal single phase region require a longer preparation time because of high viscosity (about 3 weeks), but (once prepared) do not show any changes (as judged by visual inspection and polarized optics microscopy) over 2 years of aging. The situation is slightly different for samples within the black three-phase triangle in Figure 7. When just prepared, they appear as a milky emulsion encompassing the whole volume. However, 1 month of ripening is enough to show some oil creaming and water sedimentation (the phase in between remains milky). Waiting for longer times just increases the oil and water volumes at the expense of the middle phase. On the basis of these findings, we retain that the phase behavior depicted in Figure 7 well represents the equilibrium phase diagram.

The phase diagram is dominated by the three-phase triangle water + L_α + oil. This feature and the sequence of phases along water dilution lines seem to be shared by other systems with bulky biocompatible oils:

(i) We have found consistent results using EO (water dilution of 15% and 30% of PC/EO mixtures).³⁸

(ii) The same sequence of phases might be inferred from the birefringent textures previously found at different water loading for PC/water/isopropylmyristate³⁹ (included the peculiar oil-in- L_α emulsion; compare Figure 6B with plate 3c of ref 39).

(iii) The ternary phase diagram PC/water/soybean oil recently reported⁴⁰ reveals akin phase behavior.

On the contrary, the phase behavior previously found by using cyclohexane¹⁹ and isooctane²⁷ as oils is markedly different from that outlined in Figure 7. It appears that the subtle interplay between hydration of lecithin head-groups and swelling of its lipophilic tails results in very different phase behaviors. This has interesting consequences either on our basic knowledge of lecithin self-assembly or on technical application.

The shape of self-assembled structures depends strongly on the spontaneous curvature, H_0 , of the interfacial film, and by the relative volumes of water, oil, and surfactant. Within the harmonic approximation the curvature free energy density of an interfacial film can be written as^{41–43}

$$g_c = 2\kappa(H - H_0)^2 + \bar{\kappa}K \quad (3)$$

Here, κ and $\bar{\kappa}$ are the bending rigidity and saddle splay constant and H and K are the local mean and Gaussian curvatures of the interface. Using eq 3 and taking into account the relations existing between H , K , and the relative volumes of surfactant and dispersed phase, the stability of spherical, cylindrical, and lamellar aggregates can be evaluated in closed form from eq 3 as detailed in the literature.^{42,44} The output of calculations depends on the $\bar{\kappa}/\kappa$ ratio and on the ratio between the dispersed phase volume and the interfacial area (i.e., on W_0 in the case of inverted structures). In Figure 9 are shown the stability

(38) Palazzo, G. Unpublished results.

(39) Mackeben, S.; Müller, M.; Müller-Goymann, C. C. *Colloids Surf., A* **2001**, *699*, 183.

(40) Lei, L.; Ma, Y.; Kodali, D. R.; Liang, J.; Davis, H. T. *J. Am. Oil Chem. Soc.* **2003**, *80*, 383.

(41) Helfrich, W. *Z. Naturforsch.* **1973**, *28c*, 693.

(42) Safran, S. A. *Statistical Thermodynamics of Surfaces, Interfaces and Membranes*; Addison-Wesley Publishing Company: New York, 1994; Chapter 8.

(43) Olsson, U.; Wennerström, H. *Adv. Colloid Interface Sci.* **1994**, *49*, 113.

(44) Safran, S. A. *J. Chem. Phys.* **1983**, *78*, 2073.

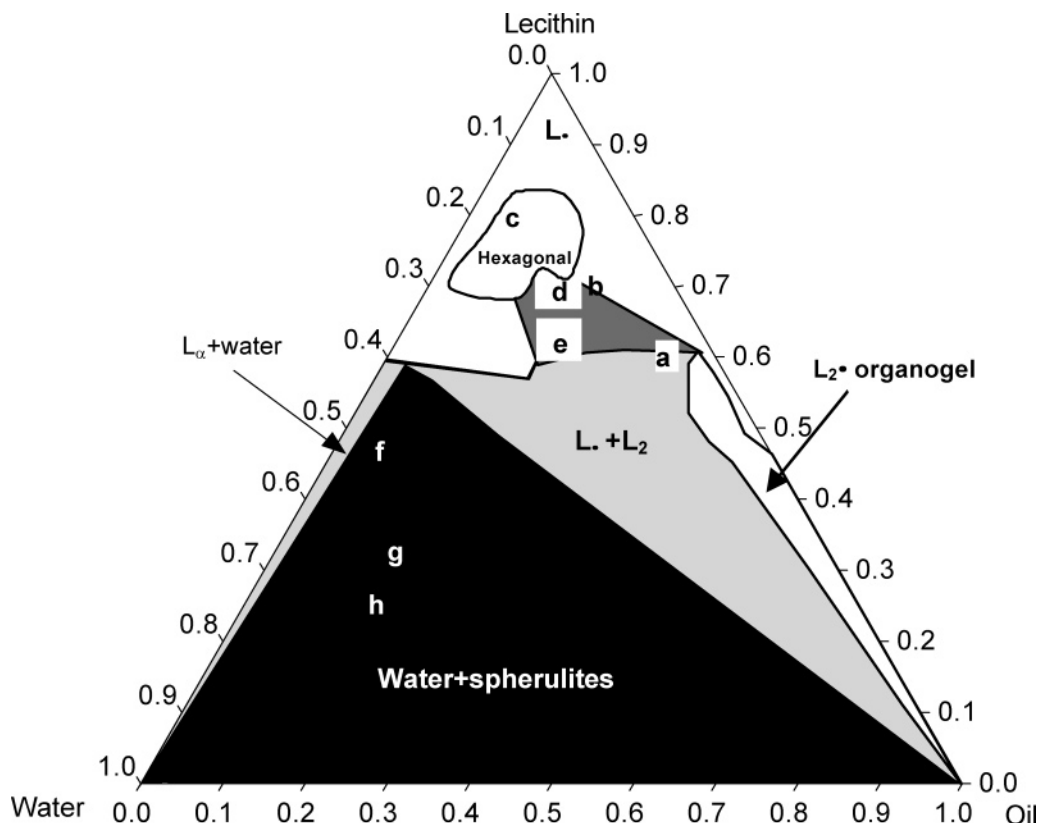


Figure 7. Phase diagram of the lecithin/water/isopropylpalmitate system: single-phase region in white; two-phase region in gray; three-phase region in black. It was obtained from observations taken after 2 years of ripening. The dark gray area denotes a complex multiphase region that was not investigated in detail. The locations of samples a–h (cf. Table 2 and Figures 4, 5, and 8) are also shown.

Table 2. First-Order Bragg Peak (q) and Repeat Distance ($d = 2\pi q^{-1}$) for Liquid-Crystalline Phases in the PC/Water/IPSP System (Figure 7)

PC (wt %)	H ₂ O (wt %)	W_0	equilibria	q (Å ⁻¹)	d (Å)	sample
60	10	7.2	$L_2 + L_\alpha$	0.123 (L_α)	51 (L_α)	a
60	20	14.3	$L_2 + L_\alpha + H$	0.0996 (H)	73 (H)	e
				0.116 (L_α)	54 (L_α)	
60	25	18	L_α	0.134	47	
70	5	3.1	L_α	0.130	48	
70	10	6.1	L_α	0.132	47	b
70	20	9.2	$H + L_\alpha$	0.057 (H)	126 (H)	d
				0.092 (L_α)	68 (L_α)	
70	20	12.3	H	0.128	60	
70	25	15.3	H	0.046	157	
80	5	2.7	L_α	0.137	46	
80	10	5.4	H	0.128	57	
80	15	8.1	H	0.113	64	c
89	6	2.9	L_α	0.138	46	

region of spheres, cylinders, and lamellae in the case of $\bar{\kappa}/\kappa = 0$, a situation likely met in the present system (where bicontinuous structures are absent). In any case the prediction of Figure 9 can be thought of as a qualitative description of the stability of different geometries upon water loading also in the case of positive $\bar{\kappa}$ values.⁴²

For highly negative H_0 (we adopt the convention of counting curvature toward water as negative) spherical reverse micelles are stable (white region in Figure 9). Their maximum size is $(1 + \bar{\kappa}/2\kappa)/H_0$, and for further water addition the system expels excess water leading to a Winsor II equilibrium between excess water and w/o droplets (light gray region in Figure 9). For small values of W_0 (or for less negative H_0) cylindrical structures are more stable (gray region in Figure 9). When the spontaneous curvature is very close to zero, locally planar films

are preferred (black region in Figure 9) resulting in a so-called Winsor III equilibrium, with bicontinuous microemulsion coexisting with excess water and oil.⁴³ The lecithin monolayer or bilayer has a high bending rigidity and does not form bicontinuous microemulsions without cosurfactant/cosolvent.⁴⁵ Instead of the microemulsion a concentrated lamellar phase is formed. Because of the high bilayer rigidity, the steric (Helfrich) repulsive force⁴⁶ is very weak and cannot overcome the attractive van der Waals force. Hence the lamellar phase does not swell with either water or oil, leaving a large three-phase triangle (water + L_α + oil) in the center of the phase diagram. There is no micellar phase on the water-rich side, while on the oil-rich side we find a narrow L_2 phase where an organogel is formed. To understand this we need to note that the spontaneous curvature is only composition independent (i.e., a true field variable) when the surfactant film is saturated with solvent. If we consider a water dilution line starting at zero water content, the film is saturated with oil, but for low water content it is not saturated with water. Addition of water will increase H_0 until the film is fully hydrated, as illustrated in Figure 9. H_0 also depends on chain length of the oil. Shorter oils penetrate the film to a higher degree,^{47–51} giving a larger negative increment to H_0 . In the case of the highly penetrating cyclohexane (qualitatively illustrated by the

(45) Shinoda, K.; Araki, M.; Sadaghiani, A.; Khan, A.; Lindman, B. *J. Phys. Chem.* **1991**, *95*, 989.

(46) Helfrich, W. *Z. Naturforsch.* **1978**, *33a*, 305.

(47) Chen, S. J.; Evans, D. F.; Ninham, B. W. *J. Phys. Chem.* **1984**, *88*, 1631.

(48) Gruen, D. W. R.; Haydon, D. A. *Pure Appl. Chem.* **1980**, *52*, 1229.

(49) Gruen, D. W. R. *Biophys. J.* **1981**, *33*, 149.

(50) Gruen, D. W. R. *Biochim. Biophys. Acta* **1980**, *595*, 161.

(51) Gruen, D. W. R. *Chem. Phys. Lipids* **1982**, *30*, 105.

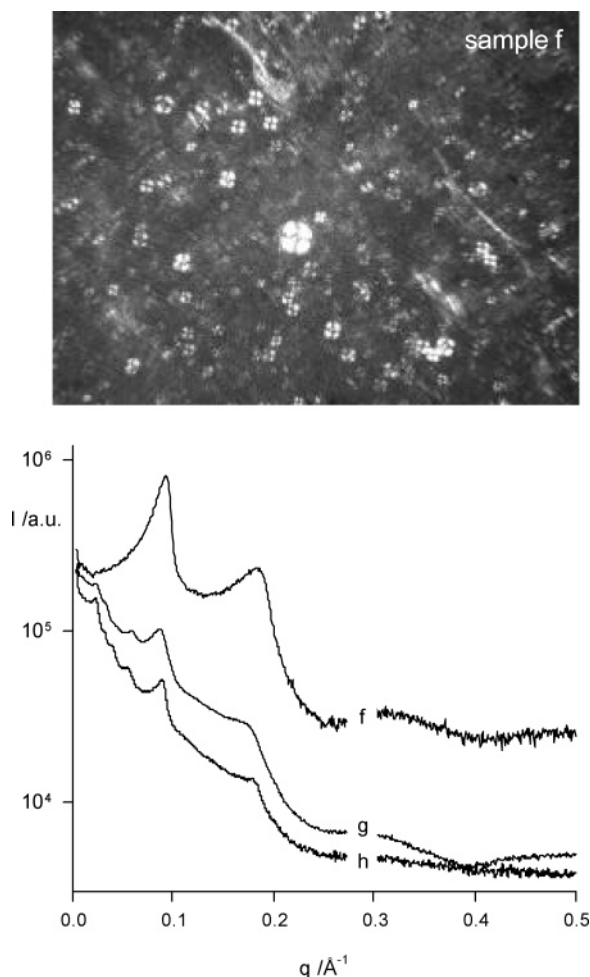


Figure 8. Samples in the spherulites region. The position of samples is shown in Figure 7; $T = 25\text{ }^\circ\text{C}$; magnification $28\times$. Upper panel: birefringence textures of sample f; note the presence of maltese crosses (spherulites) embedded in a background of oily streaks. Lower panel: SAXS curves of samples f, g, and h. Measurements were performed after 2 years of ripening.

dark curve in Figure 9), $H_0 \ll 0$ at low W_0 , resulting in small spherical reverse micelles. Upon water addition H_0 becomes less negative jumping to values where cylindrical wormlike reverse micelles are stable.²⁵ Of course, upon water loading large spherical reverse micelles reappear at higher water contents ($W_0 > 15$),²⁹ and finally for further water addition the system expels excess water leading to the Winsor II equilibrium.

In the IPP system (white curve in Figure 9) H_0 appears to be negative at very low W_0 and reverse micelles (cylindrical in shape) are stable. However as the film gets saturated with water, a lower curvature is preferred resulting in the phase transition to the lamellar phase. Due to the dependence of H_0 on the chain length of the oil, we have different phase behavior in systems with cyclohexane or fatty acid esters as oil. Fatty acid esters (IPP, EO, soybean oil) clearly behave as nonswelling oils, and the spontaneous curvature becomes null upon hydration of lecithin headgroup, so that lamellae are stable independently from the water content. Thus water loading promotes the formation of lamellae at the expense of reverse micelles. The amount of oil adsorbed by the PC tails is lower for a planar film than for a negatively curved interface, and some oil is expelled from interface leading to dilution of reverse micelles. At critical water content, all the lecithin is in the L_α phase coexisting with almost

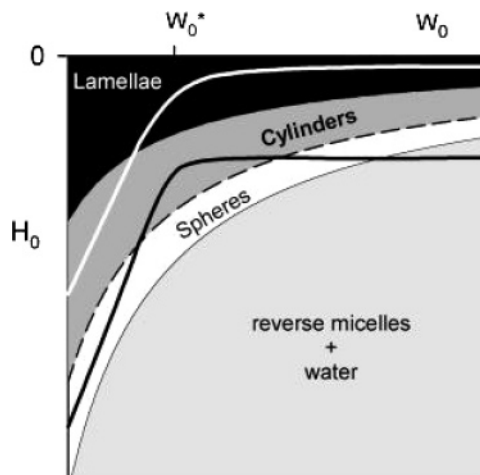


Figure 9. Schematic illustration of the stability of spherical (white), cylindrical (gray), and lamellar (black) aggregates in the variables H_0 and W_0 . The light gray region denotes the two-phase Winsor II equilibrium. Calculations were done according eq 3 assuming $\bar{\kappa} = 0$. Also sketched are the effect of an increase in H_0 upon water loading as inferred from the cyclohexane (dark curve) and IPP (white curve) phase behavior. For both oils the surfactant film is assumed to be saturated by water at $W_0 = W_0^*$.

pure oil. Subsequent water loading induces swelling of lamellae until excess water is rejected resulting in the water + L_α + oil three-phase body. Samples in this three-phase region are emulsion-like and separate only part of excess phases. The amount of water and oil has little effect on the interlamellar space (see Figure 9), suggesting that fully swollen multilamellar vesicles seclude excess phase droplets. Such hypothetical structure are expected to be very stable. Indeed the highest energy part of classical spherulites, the highly curved inner sheets,⁵² are replaced here by liquid droplets. On the other hand, the coating with multi-bilayers of a surfactant with null spontaneous curvature and high bending modulus furnishes a large energy barrier to the coalescence of both oil and water droplets,^{53–55} in agreement with the wide range of composition (from the oil to the water corner) where emulsions are found to be stable.

5. Conclusion

Upon water addition lecithin dissolved in fatty acid esters self-assembles into reverse micelles. Such aggregates are likely cylindrical (viscosity and diffusion are incompatible with a dispersion of hard-spheres). Moreover, they are not wormlike because the Newtonian behavior holds over a large shear rate interval, and the zero shear viscosity is lower than that found in wormlike systems by at least 2 orders of magnitude. In addition the echo attenuation recorded in PGSE-NMR does not show any signature of curvilinear diffusion. The presence of intermicellar branches can be safely excluded on the basis of PGSE-NMR results. As a whole, the microstructure appears to be very different from that inferred from investigation on akin systems where hydrocarbons are used as oil. Also the phase diagram for the IPP-based system is markedly different from those reported in the case of cyclohexane, decane, and isooctane as oil. The

(52) Mitchell, D. J.; Ninham, B. W. *J. Chem. Soc., Faraday Trans.* **1981**, 77, 601.

(53) Friberg, S. E.; Solans, C. *Langmuir* **1986**, 2, 121.

(54) Kabalnov, A.; Tarara, T.; Arlauskas, R.; Weers, J. J. *Colloid Interface Sci.* **1996**, 184, 227.

(55) Kabalnov, A.; Wenneström, H. *Langmuir* **1996**, 12, 276.

peculiar features of the PC/water/IPP system are a large portion of the phase diagram that is occupied by a three-phase body (water + L_α + IPP) and the absence of any Winsor II equilibria. The above-described differences in phase behavior and microstructure between fatty acid esters and hydrocarbon can be rationalized within the flexible surface model by assuming that the lecithin headgroups are fully hydrated only above a critical water-to-lecithin ratio ($W_0 = 5-8$) and taking into account the different ability of the oils to swell the lecithin tails. On the applied research perspective the three-phase triangle (water + L_α + oil) is very interesting. The water-poor side of such a triangle defines the maximum water uptake compatible with a phase separation between very diluted L_2 solution (almost pure oil) and concentrated lamellar phase. This is the water content where most of the oil can be easily recovered from the mixture, a process (degumming) widely used in refining soybean oil. On the other hand the three-phase body defines a region where emulsions are very stable. The presence of extremely stable emulsions can be detrimental or advantageous depending

on the process of interest. In the degumming process, emulsions entrap most of the oil and particular care must be done to avoid this range of composition.⁴⁰ In the case of drug delivery, the presence of stable barriers permits a slow delivery of pharmaceuticals. This is, likely, the rationale for the performance of lecithin organogels made of isopropylmyristate as carrier of timol maleate in the therapy of glaucoma.³⁹ On contact with the lachrymal fluid, a stable emulsion forms, leading to a controlled release of timol maleate.

Acknowledgment. The authors express their gratitude to Paolo De Socio for his very valuable collaboration. This work was supported by the MIUR of Italy (PRIN 2003 NANOSCIENZE PER LO SVILUPPO DI NUOVE TECNOLOGIE) and by the Consorzio Interuniversitario per lo sviluppo dei Sistemi a Grande Interfase (CSGI-Firenze). U.O. acknowledges financial support from the Swedish Research Council (VR).

LA047974F